Int. J. Electrochem. Sci., 10 **(2015)** 8437 - 8446

International Journal of
ELECTROCHEMICAL
SCIENCE
www.electrochemsci.org

Stress Corrosion Behavior of X65 Steel Welded Joint in Marine Environment

Hongxia WAN, Zhiyong LIU, Cuiwei DU[*], *Dongdong SONG, Xiaogang LI*

Corrosion and Protection Center, University of Science and Technology Beijing, Beijing 100083, China
[*]E-mail: dcw@ustb.edu.cn

Received: 19 June 2015 / *Accepted:* 30 July 2015 / *Published:* 26 August 2015

The short-term stress corrosion cracking (SCC) behavior of X65 pipeline steel welded joints in simulated deep (1000 m) and shallow sea was studied by the immersion of U-shaped bend samples, electrochemistry, and scanning electron microscope observation of fracture surfaces. Results showed that a crack existed near the fusion line in deep sea, whereas no crack occurred in shallow sea. Tafel slope and corrosion potential of welded joint was low in deep sea environment indicting there excited hydrogen evolution reactions. Cathodic polarization was controlled by both oxygen reduction and hydrogen evolution reactions in deep sea, but only oxygen reduction reactions in shallow sea. The sensitivity of the SCC of the welded joint in deep sea was higher than that in shallow sea.

Keywords: welded joint, marine environment, stress corrosion crack, electrochemistry

1. INTRODUCTION

Submarine pipelines are important equipment for deep sea oil and gas development. Over 138 strip pipelines are laid in deep sea water, and the total length of existing submarine pipelines exceeds 4000 km. According to statistics from the United States (Minerals Management Service), 690 failure cases occurred in Mexico from 1967 to 1987, with an average of over 35 accidents happening annually. To date, the laws and characteristics of pipeline corrosion have been mastered in shallow sea environment after many years of practice both local and abroad [1-3]; however, research on the corrosion behavior of pipelines in deep sea environment remains deficient. Hence, studies on material corrosion in deep sea environment have attracted considerable attention. For example, Venkatesan et al.[4]performed deep-sea corrosion tests in the Indian Ocean at depths ranging from 500 m to 5100 m for 174 days. The work focused on ferrous alloys that did not form a protective layer upon exposure to

sea water. The mild steel deep-sea results were compared with the results of shallow sea exposure tests for 68 days, and the corrosion rate was four times higher in shallow sea than that in deep sea The maximum mild steel deep-sea corrosion rate occurred at a depth of 500 m, where the dissolved oxygen profile of the Indian Ocean at the exposure location exhibited a maximum value. These studies promoted further understanding of marine corrosion. However, research on deep sea corrosion is a difficult project with high cost, high failure probability, and a long test period. Therefore, deep sea environment needs to be simulated in a laboratory. Recently, several laboratory experiments that simulated deep sea environment [5-9] were performed. The results of these experiments demonstrated that hydrostatic pressure was an ineligible aspect to material corrosion; the susceptibility of corrosion was increased under high hydrostatic pressure.

However, deep sea environment is not only characterized by high hydrostatic pressure (which increases by 1 atm for every depth of 10 m), but also by low oxygen and temperature [10]. In this environment, the uniformity corrosion of pipelines is inhibited and the effect of hydrogen permeation is enhanced. All these factors can increase the likelihood of localized corrosion [6, 11]. As we all know, localized corrosion often transform into SCC. Meanwhile, the welded joint is the most corrosion-sensitive part [12-15]. Some studies [16-18] have indicated that the welded joint of X65 pipeline steel can easily undergo corrosion. In some conditions, welded joint corrosion frequently evolves into stress corrosion cracks during the corrosion process [19], which is one of the vital threats to safety of pipeline operation [20], and significant failures in natural oil/gas transmission pipelines have been found throughout the world. X65 pipeline steel widely used in oil transport in marine environment. However, to date, few studies have been performed on the behavior and mechanisms of the stress corrosion of X65 steel welded joints in marine environments; the occurrence and expansion mechanism of stress corrosion remains unclear. Consequently, studies on theory of stress corrosion in deep sea environment are important. Such works can provide bases for the protection and safety evaluation of the stress corrosion of pipeline steel in deep sea environment. Consequently, it is important to study the behavior and mechanism of X65 steel welded joint in marine environment. In this work, U-shape bend immersion tests, electrochemical measurements and surface analysis techniques were used to investigate the SCC behavior and mechanism. And the sensibility of stress corrosion is discussed.

2. EXPERIMENT

2.1 Materials

The test specimens were cut from cyclic annular welded joints (with air cooling after automatic argon arc welding) of submarine pipeline steel. Table 1 shows the chemical composition of the matrix and the welded joint of the pipeline.

Table 1. Chemical composition of X65 pipeline steel (wt%)

	C	Si	Mn	P	S	Ni	Cu	Mo	N	Nb	Al	Ti	Cr	Ni	Fe
M	0.05	0.17	1.51	0.021	0.005	0.013	0.03	0.01	0.006	0.06	0.02	0.02	-	-	balance
WJ	0.07	0.18	1.85	0.024	0.004	0.025	0.03	0.01	0.006	0.06	0.02	0.02	0.41	0.12	balance

2.2 Test solution

A 3.5% NaCl (wt%) solution was used as the mother solution, with the pH of the solution regulated by NaOH (pH value of the solution was 7.5). Different depths of marine environments were simulated by controlling dissolved oxygen level, temperature, and pressure. A deep sea depth of 1000 m and shallow sea environment were simulated. The parameters are given in Table 2.

Table 2. Parameters of the simulated deep sea and shallow sea environments

	Pressure	Dissolved oxygen	Temperature
Deep sea/1000 m	10 MPa	2 mg/L	4 °C
Shallow sea	0.1 MPa	7 mg/L	25 °C

2.3 Metallographic test

Metallographic specimens with a weld zone (WZ) at the center were cut from the welded joint with an area of 35 mm × 10 mm × 5 mm. The surfaces of the specimens were successively polished with 2000 grit emery paper until they were as bright as a mirror and without any scratch. Then, the specimens were rinsed with distilled water and ethanol, and etched with 4% nitric acid alcohol solution. After dry cleaning, the microstructure of each metallographic specimen was observed under a microscope. After etching, the organizations of WZ and the heat-affected zone (HAZ) were obviously different. The length of WZ was 10 mm, whereas that of HAZ was approximately 4 mm.

2.4 U-shaped bend immersion test and morphological observation

A U-shaped bend was also cut from the welded joint, with WZ in the middle of the specimen. The U-shaped bend samples were prepared according to the GB/T15970.3 specification. Sample surfaces were burnished parallel to the tension direction to 2000 grits before cleaning in distilled water and acetone.

Each U-shaped bend was immersed for 720 h in simulated deep or shallow sea water. After immersion, the mechanical parts were cut from the U-shaped bend using a hand saw and then cleaned in acetone. The corrosion product that formed on the sample was thoroughly removed using a descaling solution that contained 500 mL HCl (special gravity, 1.189), 500 mL distilled water, and

3.5g hexamethylenetetramine. After rinsing and drying, specimen morphology was observed via scanning electron microscopy (SEM; Quanta 250).

2.5 Electrochemical measurement

Based on the results of the metallographic experiment, an electrochemical specimen of WZ and the basis metal was cut from the welded joint and HAZ with sizes of 10 mm × 10 mm × 4 mm and 10 mm × 4 mm × 4 mm, respectively. Electrochemical tests were conducted on a PARSTAT2273 electrochemical workstation with a three-electrode cell system, in which the specimens were used as the working electrode, Ag/AgCl as the reference electrode, and a platinum plate as the counter electrode. Prior to measurement, the working electrode was maintained for 30 min in the solution to ensure that a steady state value of the corrosion potential was reached. Electrochemical impedance spectroscopy (EIS) was measured at the AC voltage disturbance of 10 mV, with a test frequency ranging from 100 KHz to 10 mHz. Potentiodynamic polarization curves were measured at a potential sweeping rate of 0.5 mV/s at a relatively open circuit potential from−0.5 V (vs. SCE) to 0.5 V (vs. SCE).

3. RESULTS

3.1 Microstructure of welded joint of X65 pipeline steel specimen

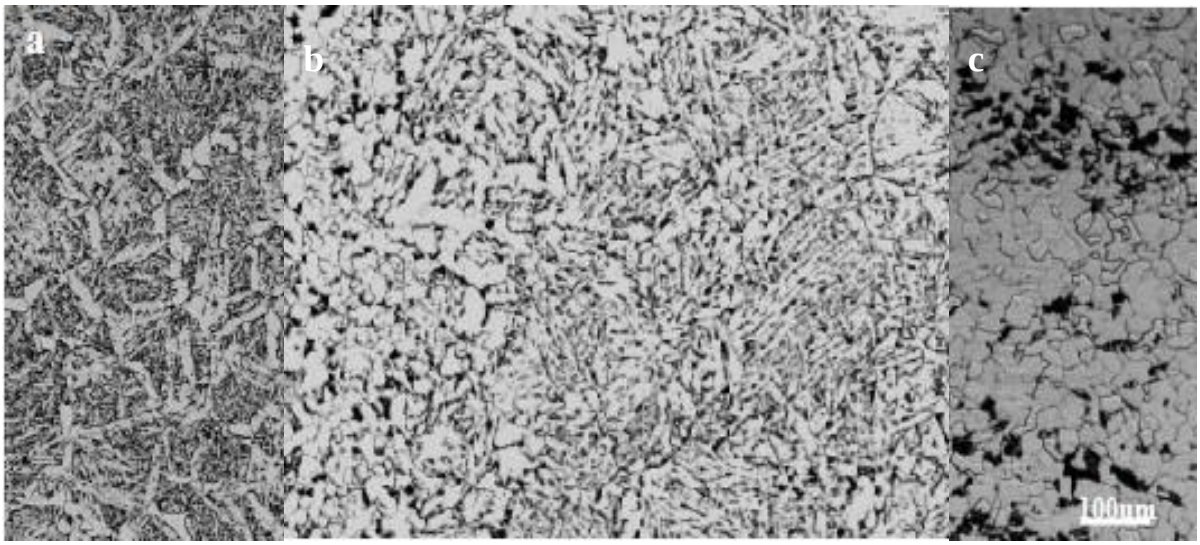

Figure 1. Metallograph of the welded joint of X65 pipeline steel: (a) WZ, (b) HAZ, and (c) the matrix

Figure 1 shows the metallographic sample of the welded joint of X65 pipeline steel in (a) WZ, (b) HAZ, and (c) the matrix. The microstructure of the weld zone of X65 steel is mainly composed of pearlite, flake ferrite, and acicular ferrite (Figure 1a). Flake ferrite is distributed at grain boundaries and acicular ferrite is distributed in grain internal regions. The tissue morphology satisfies the

Widmanstatten structural features, and the grain is relatively bulky. The microstructure of HAZ is mainly composed of polygonal ferrite, pearlite, and bainite with uneven size organization (Figure 1b), whereas the microstructure of the matrix steel is mainly composed of polygonal ferrite and pearlite (Figure 1c). Compared with those of WZ and HAZ, the microstructure of the matrix is relatively small and presents banded structural characteristics.

3.2 Results and analysis of the immersed U-shaped bend

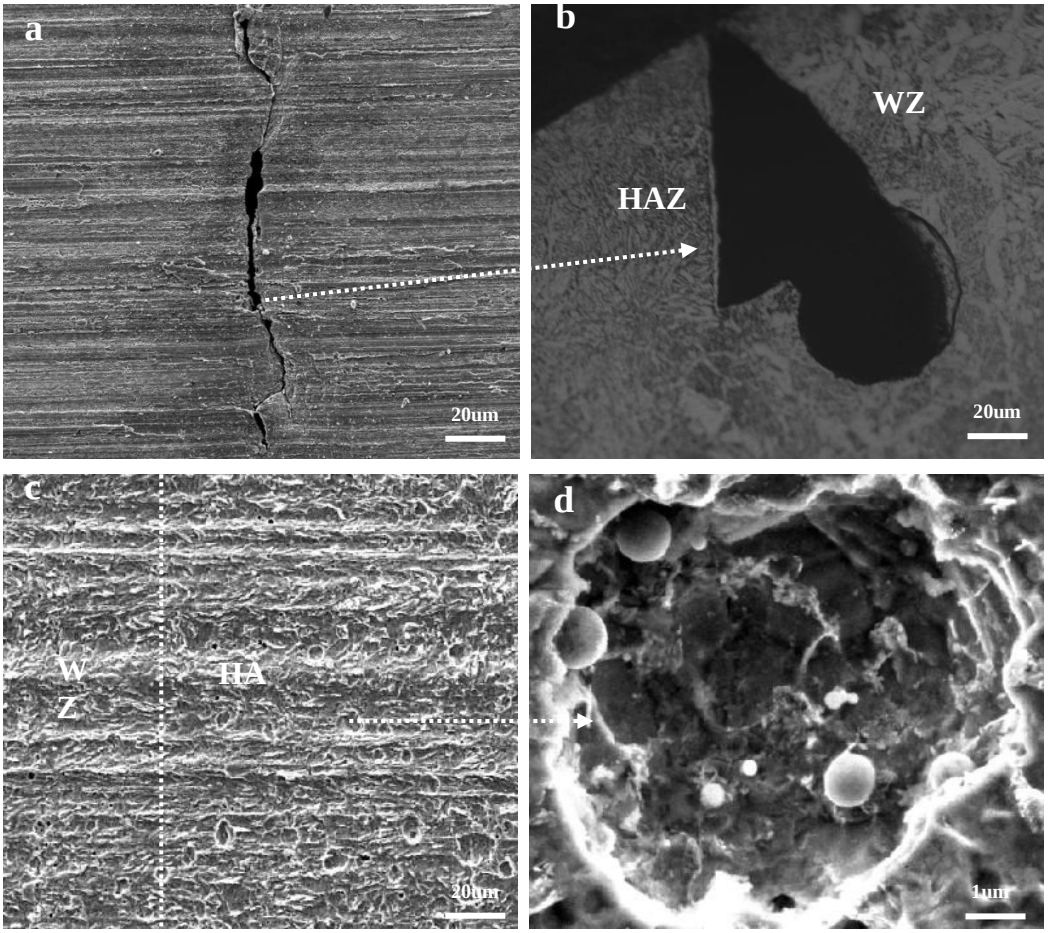

Figure 2. SEM images and metallograph of the U-shaped bend sample of X65 pipeline steel welded joint immersed for 720 hours in (a–b) simulated deep and (c–d) shallow sea environments

Figure 2 shows the micromorphology of the U-shaped bend of the welded joint of X65 steel in deep and shallow sea environments. In deep sea environment, the crack was generated in the fusion line of the U-shaped bend. One side of crack was a metallograph of WZ, and the other side was a metallograph of HAZ (Figure 2b). However, when the samples were immersed in shallow sea environment, cracks were not produced but pits were present; no sign of stress corrosion cracking (SCC) initiation was found inside the pits, which might be attributed to the low oxygen level in the deep sea environment. Therefore, the oxygen reduction reaction was restrained, whereas the hydrogen evolution reaction was strengthened. In addition, bainite was present in the fine-grain region of HAZ,

which was highly sensitive to hydrogen embrittlement.[19] The absence of cracks in shallow sea samples indicated the lower sensitivity of SCC in shallow sea, whereas cracks in deep sea samples indicated the higher sensitivity of SCC in deep sea environment. However, in terms of uniform corrosion, that of the welded joint in shallow sea environment was more serious because of oxygen corrosion. In shallow sea environment, the corrosion of WZ (Figure 2c) was uniform with some pits. By contrast, more pits were found in HAZ (Figure 2c), which might be a result of the high activity of HAZ organization. The electrochemical method was used to prove that HAZ activity was higher than those of WZ and the matrix, whereas the SCC sensitivity of the welded joint in deep sea was higher than that in shallow sea.

3.3 Electrochemical results and analysis

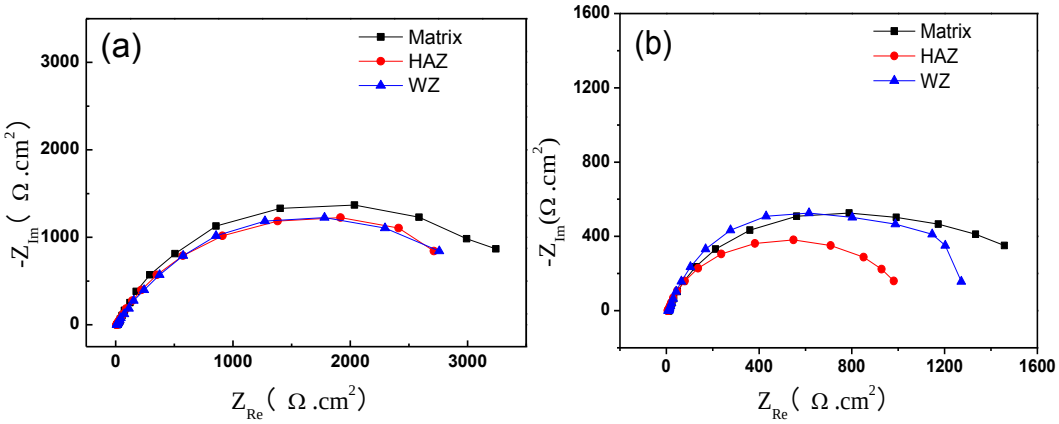

Figure 3. Simulated (a) deep sea and (b) shallow sea EIS of the X65 pipeline steel welded joint

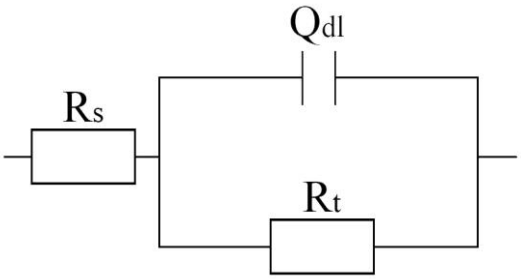

Figure 4. Equivalent EIS circuit of the X65 pipeline steel welded joint

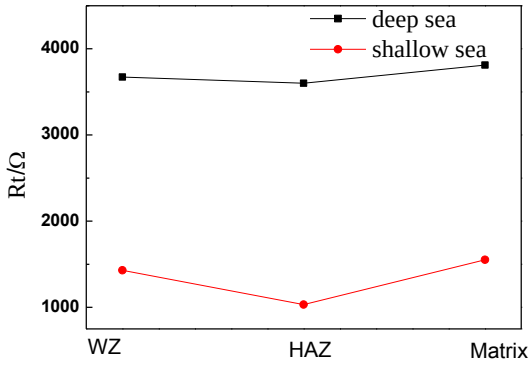

Figure 5. Impedance fitting of the X65 pipeline steel welded joint in simulated deep sea and shallow sea environments

Figure 3 shows the EIS of the welded joint of X65 pipeline steel in simulated deep sea (a) and shallow sea (b) environments. The EIS only exists at a time constant of the capacitive reactance arc. Figure 4 is the fitting circuit model where R_s represents the resistance, Q_{dl} represents the constant phase angle element reacting to the electric double layer capacitor, and R_t shows the charge transfer resistance. The fitting result of R_t is presented in Figure 5. This figure shows that the R_t values of the welded joint in deep sea environment were greater than those in shallow sea environment, which explained that the corrosion rate in deep sea environment was lower than that in shallow sea environment. This finding is similar to those of previous work[4]. However, the dissolved oxygen level was low in deep sea environment, and hydrogen evolution reaction was strengthened, which made the joint prone to hydrogen embrittlement or hydrogen induced cracks. Furthermore, the R_t values of HAZ in deep and shallow sea environments were lower than those of WZ and the matrix. These results suggested that the electrochemical activity of HAZ was higher, and corrosion was more severe than in other areas. In some conditions, corrosion might have induced the development of SCC in HAZ[18]. For example, the U-shaped bend immersed in deep sea environment produced cracks in the fusion line of HAZ.

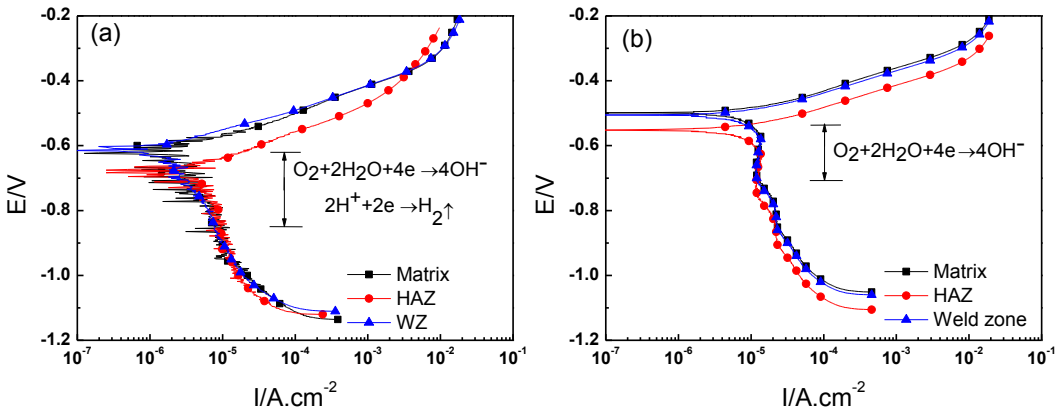

Figure 6. Polarization curves of X65 pipeline steel obtained under simulated (a) deep sea and (b) shallow sea environments

Table 3. Corrosion potential, corrosion current density and Tafel slopes of X65 pipeline steel in the simulated deep sea and shallow sea environments

Environments and Materials		Ecorr/V	Icorr/μA.cm^{-2}	ba(mV.dec^{-1})	bc(mV.dec^{-1})
Deep sea environment	WZ	-0.6086	2.35	127	76.5
	HAZ	-0.6774	4.80	132	83.7
	Matrix	-0.6231	2.86	120	86.4
Shallow sea environment	WZ	-0.4967	8.60	30.2	205.6
	HAZ	-0.5516	9.83	40.9	209.8
	Matrix	-0.5045	8.12	34.6	210.2

Figure 6 shows the polarization curves of WZ, HAZ, and the matrix of the X65 pipeline welded joint in simulated deep sea and shallow sea environments. And table 3 is corrosion potential, corrosion current density and Tafel slope of the fitting of Figure 6 data. As shown in table 3, the anode Tafel slope of polarization curves of welded joint is not particularly different, but the value of which in deep sea environment is greater than that in shallow sea. The anodic dissolution of X65 pipeline was inhibited and cathodic reaction was promoted the in deep sea environment. the cathode Tafel slope of polarization curves of welded joint is not less than 118mV in deep sea environment, which is the limit value of Tafel slope of hydrogen evolution mechanism [22]. However, in shallow sea environment, Tafel slope of polarization curves of welded joint is about 200mV above 118mV. Meanwhile, given the lower oxygen levels in deep sea environment, the corrosion potential of the welded joint in deep sea environment was lower than that in shallow sea environment, which can reach the hydrogen evolution potential. Therefore, hydrogen evolution reactions occurred in deep sea environment. Thus, Cathodic polarization was controlled by the mixture in deep sea environment and by oxygen diffusion in shallow sea environment. Therefore, oxygen reduction and hydrogen evolution reactions were present in deep sea environment, but only oxygen reduction reactions occurred in shallow sea environment. In deep sea environment, low oxygen levels promote hydrogen evolution reactions, the SCC sensitivity was high and it can easily cause SCC. These results are similar to those of the immersed U-shaped bend (Figure 2) From corrosion potential in table 3, in both deep sea and shallow sea environments, the corrosion potential of HAZ was the lowest, whereas those of the matrix and WZ were higher, which indicated that a galvanic effect occurred among the matrix, HAZ, and WZ. HAZ is the anode and the other zones function as the cathode. In terms of corrosion current density, that of HAZ was greater than those of other zones in both deep sea and shallow sea environments (Table 3). All these results suggested that HAZ activity was higher than those of the other zones and HAZ would be priority to corrosion. Which was in accordance with the EIS results (Figures 3 and 5).

4. DISCUSSION

Given that a shallow water environment is an open system, oxygen will be fully dissolved in water, and the anode reaction process is as follows:

$$Fe + 2OH^- \rightarrow Fe(OH)_2\downarrow + 2e. \quad (1)$$

The cathode reaction process may exhibit the following response:

$O_2 + 2H_2O + 4e \rightarrow 4OH^-$. (2)

The anodic reaction in deep sea environment is similar with that in shallow sea environment. However, dissolved oxygen concentration is greatly reduced in deep sea; thus, the depolarization processes of oxygen and hydrogen occur in the cathode reaction. Consequently, the cathodic reaction has a depolarization process of H^+, that is,

$H^+ + e \rightarrow H_{abs}$, $H_{abs} \leftrightarrow H_{ads}$, $2H_{abs} \rightarrow H_2\uparrow$. (3)

Given the hydrostatic pressure, the generated hydrogen adsorption easily spreads into the base metal, which can cause hydrogen embrittlement and hydrogen-induced cracking, as well as promote the initiation and development of SCC.

In deep sea environment, the Tafel slope of polarization curves of welded joint is less than 118mV (Table 3) and the corrosion potential of the welded joint is low, which indicts that there exists hydrogen evolution reactions [22]. Thus, cathodic polarization in deep sea environment is controlled by a mixture of oxygen reduction and hydrogen evolution reactions (Figure 6a). There have been extensive evidences [23, 24] indicating that hydrogen plays an important role in near-neutral pH SCC in pipelines. In addition, low oxygen in deep sea environment would promote the hydrogen evolution reaction, some part of hydrogen adsorb on the electrode surface and spread into the base metal, which can reduce corrosion resistance and the cohesion strength of the metal lattice and make these areas local brittlement, thus, hydrogen will be reinforced stress corrosion susceptibility in deep sea environment. For the organization, bainite is present in HAZ (Figure 1b), and thus, hydrogen embrittlement resistance is low [21]. The welded joint has a high cooling rate during the welding process, and WZ has high density of lattice defects, which increases activities in WZ and HAZ. The temperature gradient of the welding process can produce welding residual stress, which is sometimes high, and may reach the yield limit. Local stress intensity will strengthen local dissolution, which forms a permanent slip band in steel and enhances the activity of the matrix around the welded joint[25]. Given the change in microstructural and mechanical properties resulting from the welding thermal cycle, HAZ will exhibit local hardening and become brittle and less ductile, which improves the SCC sensitivity of HAZ under welding residual tensile stress. Therefore, the SCC sensitivity of the welded joint in deep sea environment is high and prone to SCC. Given the sufficient oxygen level in shallow sea environment, cathodic polarization is controlled by oxygen diffusion (Figure 6b). The U-shaped bend of corrosion products is more than that in deep sea environment, but SCC sensitivity is low without any SCC. The Rt value and corrosion potential of HAZ are lower than those of WZ and the matrix (Figure 5), which indicates that the activity of HAZ organization is high and a galvanic effect exists, such that HAZ is the anode with more pits. This result is attributed to the metallurgical phase transition of the welded joint and HAZ during welding, which significantly changes inherent corrosion behavior, for example, to produce bainite in HAZ (Figure 1b). Compared with ferrite and pearlite, bainite has high hardness, which increases its sensitivity to corrosion. Within a certain period, corrosion may induce the initiation and development of HAZ SCC.

5. CONCLUSION

Cracks were generated near the fusion line of the U-shaped bend in deep sea environment but no crack was produced in shallow sea environment. SCC sensitivity in deep sea environment was higher than that in shallow sea environment. Tafel slope and corrosion potential of welded joint is low in deep sea environment indicting there existed hydrogen evolution reactions and cathodic polarization of X65 steel welded joint was controlled by a mixture of oxygen reduction and hydrogen evolution reactions in deep sea environment but only by oxygen diffusion reactions in shallow sea environment, which showed high SCC sensitivity in deep sea environment.

ACKNOWLEDGEMENTS
The authors are grateful for the financial support from National 973 Basic Research Program of China (No.2014CB643300), the National Natural Science Foundation of China (No.51171025, 51471034,51371036), and Beijing Higher Education Young Elite Teacher Project.

References

1. M. Schumacher, *Seawater corrosion handbook*, Noyes Data Corp, United States, 1979.
2. S. Dexter, *Handbook of oceanographic materials*, New York: John Wiley and Sons, 1979.
3. K.A. Chandler, *Marine and Offshore Corrosion: Marine Engineering Series*, Elsevier, 2014.
4. R. Venkatesan, M. Venkatasamy, T. Bhaskaran, E. Dwarakadasa, M. Ravindran, *Brit Corros J*, 37 (2002) 257-266.
5. T. Zhang, Y. Yang, Y. Shao, G. Meng, F. Wang, *Electrochim Acta*, 54 (2009) 3915-3922.
6. Y. Yang, T. Zhang, Y. Shao, G. Meng, F. Wang, *Corros Sci*, 52 (2010) 2697-2706.
7. B. Liu, T. Zhang, Y. Shao, G. Meng, J. Liu, F. Wang, *Int. J. Electrochem. Sci*, 7 (2012) 1864-1883.
8. A. Beccaria, G. Poggi, G. CASTELLO-2, *Brit Corros J*, 30 (1995) 283-287.
9. S. Chen, W. Hartt, *Corrosion*, 58 (2002) 38-48.
10. P. Traverso, E. Canepa, *Ocean Eng*, 87 (2014) 10-15.
11. M. Raoof, T.J. Davies, *Int J fatigue*, 30 (2008) 2220-2238.
12. C. Du, X. Li, P. Liang, Z. Liu, G. Jia, Y. Cheng, *J mater eng perform*, 18 (2009) 216-220.
13. C. Garcia, F. Martin, P. De Tiedra, Y. Blanco, M. Lopez, *Corros Sci*, 50 (2008) 1184-1194.
14. S. Bordbar, M. Alizadeh, S.H. Hashemi, *Mater Design,*, 45 (2013) 597-604.
15. D.-j. KONG, Y.-z. WU, L. Dan, *J Iron Steel Res Int*, 20 (2013) 40-46.
16. J. Bulger, B. Lu, J. Luo, *J mater sci*, 41 (2006) 5001-5005.
17. G. Van Boven, W. Chen, R. Rogge, *Acta Mater*, 55 (2007) 29-42.
18. L. Xu, M. Li, H. Jing, Y. Han, *Int. J. Electrochem. Sci*, 8 (2013) 2069-2079.
19. M. Sun, K. Xiao, C. Dong, X. Li, P. Zhong, *Aerosp Sci Technol*, 36 (2014) 125-131.
20. I.-u.-H. Toor, *Int. J. Electrochem. Sci*, 9 (2014) 2737-2755.
21. Z. Liu, G. Zhai, X. Li, C. Du, *J mater sci & technol*, 25 (2009) 169.
22. D.Li, *Principles of Electrochemistry*, Beijing aerospace university press, Beijing ,1987.
23. A. Marshakov, V. Ignatenko, R. Bogdanov, A. Arabey, *Corros Sci*, 83 (2014) 209-216.
24. M. Javidi, S.B. Horeh, *Corros Sci*, 80 (2014) 213-220.
25. G. Zhang, Y. Cheng, *Corros Sci*, 51 (2009) 1714-1724.